Crayfish Escape Behavior and Central Synapses.
III. Electrical Junctions and Dendrite
Spikes in Fast Flexor Motoneurons

ROBERT S. ZUCKER

Department of Biological Sciences and Program in the Neurological Sciences, Stanford University, Stanford, California 94305

THE LATERAL giant fiber is the decision fiber for a behavioral response in crayfish involving rapid tail flexion in response to abdominal tactile stimulation (27). Each lateral giant impulse is followed by a rapid tail flexion or tail flip, and when the giant fiber does not fire in response to such stimuli, the movement does not occur.

The afferent limb of the reflex exciting the lateral giant has been described (28), and the habituation of the behavior has been explained in terms of the properties of this part of the neural circuit (29).

The properties of the neuromuscular junctions between the fast flexor motoneurons and the phasic flexor muscles have also been described (13). They are facilitating and transmit reliably at repetition rates above 10 Hz, leading to repeated twitches in the fast flexor musculature. Only one neuromuscular junction, that of the motor giant, fatigues on repeated activation at about 1 Hz (3). After only a few motoneuron spikes, the junction fails and its small contribution to muscle tension is lost.

The present paper considers the last remaining point in the neural circuit mediating this behavior—the activation of the fast flexor motoneurons by the lateral giant. The only such junction studied in detail is the synapse between the lateral giant and the motor giant neurons (7). This junction occurs between the crossing axons near the point at which the motoneuron exits from the ventral nerve cord via the third root; it is electrical, and exhibits rectification. The other junctions between the giant fibers

and fast flexor motoneurons are located in the dorsal neuropil of each abdominal ganglion. Dye injections and anatomical reconstructions of identified motoneurons reveal that only those motoneurons which have dentritic branches in contact with a giant fiber are activated by that giant fiber (12, 21). All of the fast flexor motoneurons are excited by the ipsilateral giant; all but F4, F5, and F7 are also excited by the contralateral giant (21a).

The excitation of these motoneurons, seen as depolarizing potentials in their somata, does not always reach threshold for generating a spike which propagates out the axon to the periphery (14). Indeed, only the motoneurons supplying the transverse muscles (F2 and F8; ref 21a) are always effectively excited by the lateral giant, while some others (e.g., F3, F6, F9) are usually, but not always, effectively excited by the giant. This lability leads to some variability in the form and strength of the tail flexion generated by the lateral giant.

The excitation of nongiant fast flexor motoneurons by the lateral giant has been analyzed in the experiments to be reported here. The results indicate that the synapses are electrical and that the excitatory postsynaptic potentials (EPSPs) are amplified by dendrite spikes.

This mode of activation of motoneurons contrasts with the usual properties of electrically transmitting synapses. Such junctions often mediate one-for-one driving of postsynaptic neurons by presynaptic cells (2, 7). In the crayfish fast flexor motoneurons, however, the synapses are located some distance from the main axon. They

can only elicit axon spikes by first exciting spikes in the dendritic tree. These dendrite spikes then encounter a region of low safety factor at the point where the dendrites and soma process join the main axon. At moderate stimulation frequencies (above 20 Hz), the dendrite spikes may fail at this point. Thus the motoneurons display a lability in transmission that is usually associated with chemically activated neurons. By this arrangement, dendrite spikes serve an important integrative function, and may act similarly in a variety of vertebrate neurons (ref 9, p. 220).

METHODS

Crayfish (*Procambarus clarkii*) were maintained and prepared for experiments as described in the first paper in this series (28). The abdomen was pinned ventral side up in cold saline and the nerve cord was exposed and illuminated with transmitted light. The third root of the second, third, or fourth segment was exposed laterally by removing the overlying ventral cuticle and superficial flexor muscles. The root and its peripheral branches were uncovered by cutting away the second head of the anterior

oblique flexor muscle (13). Single identified fast flexor motoneurons could be selectively stimulated by placing electrodes on particular branches of the third root, and taking advantage of the unique branching pattern of each motoneuron (21a). Antidromic impulses were often monitored by placing a second electrode proximally on the third root. Orthodromic shocks were delivered to the lateral giant axon, which was dissected free from the ventral nerve cord in the last abdominal connective. Recordings were made from motoneuron somata or their processes in dorsal neuropil, using 3 M KCl microelectrodes and a Wheatstone bridge circuit. The stimulating and recording apparatus was as described earlier, as were procedures for penetrating identified elements in neuropil and calculating the arrival time of impulses in presynaptic cells in a ganglion (28, 29).

In order to study the responses of a neural model to spikes blocking in different portions of a motoneuron, identified motoneuron axons were penetrated in the third root and spikes were recorded on a Lockheed FM instrumentation tape recorder (Edison, N.J.). Each spike waveform was necessarily preceded by a stimulus artifact. In order to avoid driving the model with artifacts, the recorder output was fed into a gated linear amplifier, and the amplifier was
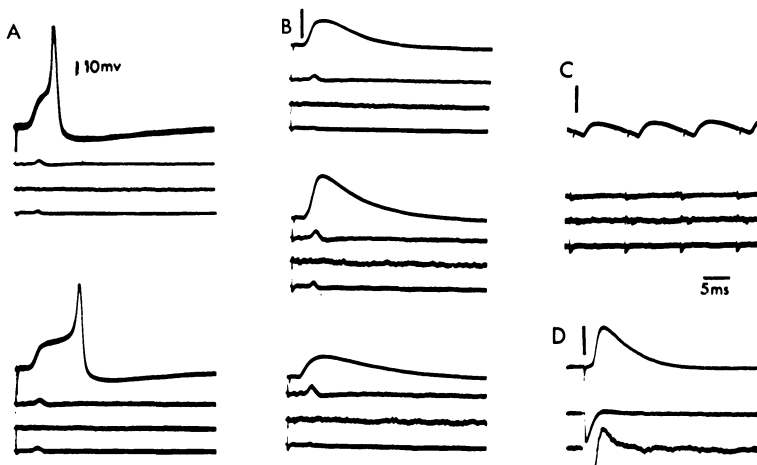
FIG. 1. Soma potentials recorded from fast flexor motoneuron F3 in the third abdominal ganglion. First trace, intracellular record. Branches of the ipsilateral third root to the posterior oblique, and the first and third heads of the anterior oblique muscles are recorded in the second, third, and fourth traces, respectively. A, B, and C are orthodromic responses after several seconds of stimulation of the ipsilateral lateral giant axon in the 5/6 connective, at frequencies of 0.5, 25, and 100 Hz, respectively. Active spike invades soma only at low frequencies (A). In B, the middle set of traces show a large soma potential correlated with an axon spike in F3, whose peripheral process innervates only the third head of the anterior oblique muscle, and consequently is recorded in the fourth trace. Spikes in other motoneurons, whose axons are monitored in the second and third traces, are not associated with activity in soma F3. C: at high frequencies of orthodromic stimulation, F3 consistently fails to generate axon spikes. D: antidromic stimulation of F3 via the third root branch previously recorded as the fourth trace. The subthreshold soma potentials in B-D were the largest observed in these experiments.

controlled by a pulse triggered by the signal and delayed sufficiently to prevent the artifact from passing through the amplifier. Thus the spike waveform was isolated from the shock artifact. Potentials generated by the model were recorded with a Bioelectric high-impedance amplifier (Hastings-on-Hudson, N.Y.).

RESULTS

Lateral giant excitation of fast flexor motoneurons

Wiersma (25) showed that each spike in a medial or lateral giant fiber excites impulses in the motoneuron axons recorded in the third root of an abdominal ganglion, and Takeda and Kennedy (13, 22) reported the presence of depolarizing potentials in the motoneuron somata in response to giant fiber stimulation. Some of the properties of these soma potentials and their relation to axon spikes recorded in the third root are illustrated in Figs. 1 and 2, recorded from the soma of fast flexor motoneuron number 3 (F3) in two preparations.

Occasionally, a full overshooting impulse is observed in the soma (component 3, ref
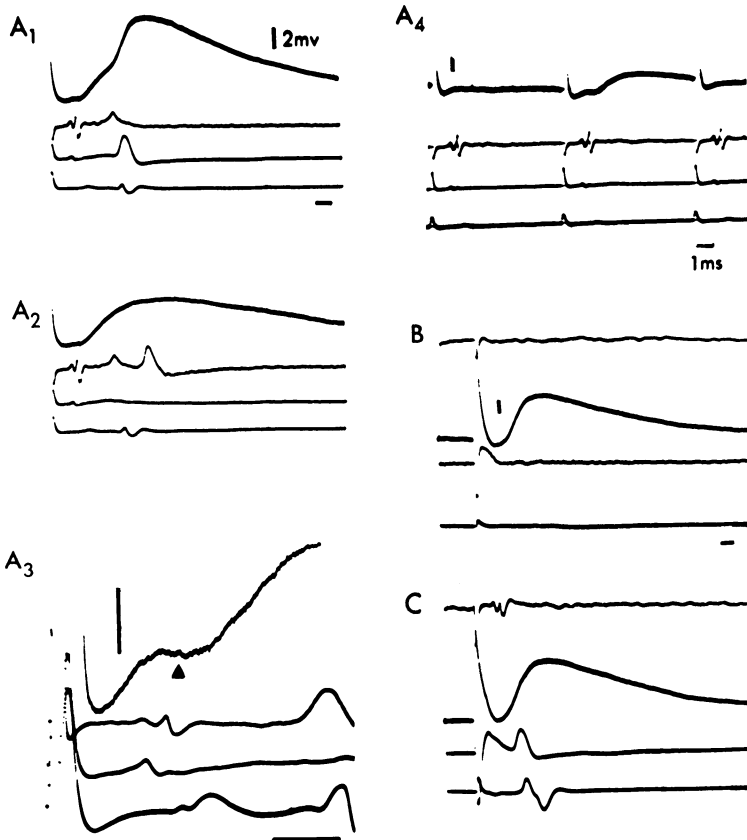
FIG. 2. F3 soma potentials from the third ganglion of a different animal. *A:* examples of typical responses to orthodromic stimulation of the ipsilateral giant in the 5/6 connective. First trace, intracellular record. Second and third traces are from the contralateral and ipsilateral third roots of the same segment; last trace is from the ipsilateral root of the next anterior segment. The triangle in trace 1 marks the arrival of the lateral giant impulse in the third ganglion. The peripheral axon spike in F3 (large spike in the third trace) correlates with the large soma potential present only in A_1. Spikes in other motoneurons monitored in the second and fourth traces have no correlates in the soma potentials of F3. Stimulus repeated at 1 Hz, except in A_4, where frequency is 100 Hz. *B:* antidromic stimulation of F3 via the third root branch previously recorded as the third trace, which is here deleted. Top trace is from the lateral giant axon in the 5/6 connective. Traces 2 through 4 correspond to traces 1, 2, and 4 of *A*. *C:* intense stimulation of contralateral third root previously recorded in second trace, which is here deleted. Top trace records the lateral giant axon; traces 2 through 4 correspond to traces 1, 3, and 4 of *A*. Current spreads to the lateral giant, exciting it directly and eliciting orthodromic soma and third root potentials.

22), following electrical stimulation of the ipsilateral lateral giant (Fig. 1*A*). Usually this spike is not seen, and a smaller, slower depolarization is recorded. At low repetition rates (about 1–5 Hz), this slow depolarization (component 2 of ref 22) corresponds one-to-one with a spike in the axon of the motoneuron. At somewhat higher rates of stimulation (10–40 Hz), this slow depolarization of the soma drops out to some stimuli in all-or-none fashion, and the axon spike recorded from that branch of the third root which contains the axon of F3 is also missing (Figs. 1*B* and 2*A*). Since this slow depolarization of the soma always corresponds to the presence of a spike in the peripheral axon, this component will be called the axon spike, as seen from the soma. The axon spike may also always be recorded from the soma after antidromic stimulation of the motoneuron in the third root (Figs. 1*D* and 2*B*). The smaller potential (component 1, ref 22) that remains after loss of the axon spike at high rates of stimulation of the lateral giant (above 50 Hz) is the main subject of this section.

In some cells, this smaller potential (component 1) reliably follows long trains of orthodromic stimulation delivered at high fre-quency (100 Hz) (see Fig. 1*C*). In other cases, it too drops out in all-or-none fashion, and an even smaller underlying potential may or may not be discernible. When this last small underlying potential is observed, it cannot be blocked at any frequency (Fig. 2*A*$_4$). All of the above types of soma potentials appear to rise from the base line with a latency of about 0.2–0.4 msec from the moment of arrival of the lateral giant spike in the ganglion recorded (Fig. 2*A*$_3$).

This apparent synaptic delay of the soma potentials and the lability of transmission at moderate frequencies (above 30 Hz) have led to speculation that the lateral giant excitation of the nongiant fast flexor moto-neurons may be chemically mediated, in contrast to the electrotonic excitation of the motor giant (10, 14, 22). However, Takeda and Kennedy (22) found that strong hyper-polarization of the soma by current injec-tion often blocked component 1 of the soma potential, unlike any chemical EPSP. They tentatively identified this potential as an electrotonically conducted dendritic branch spike, and left the issue of the nature of the synapse unresolved.

The question was approached using tech-niques developed to record from processes
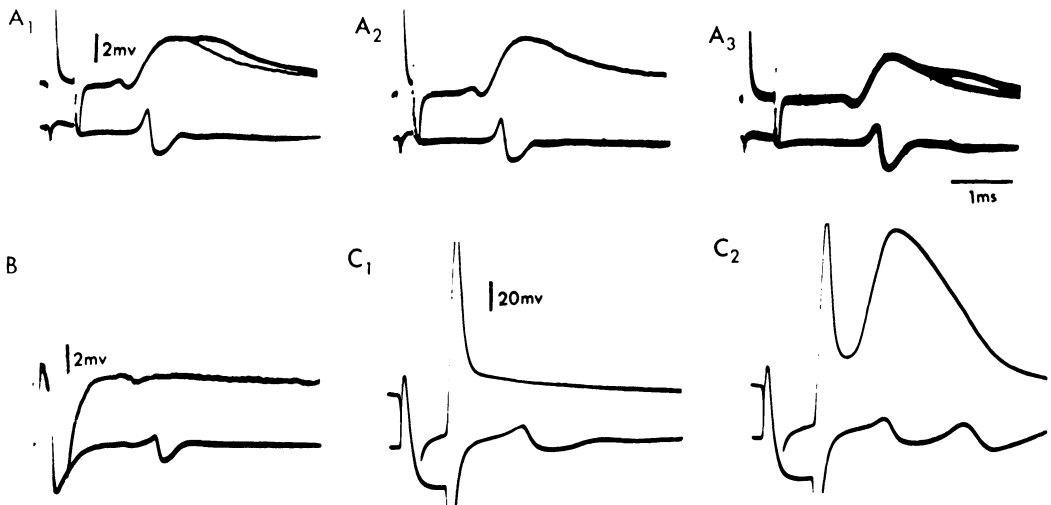
FIG. 3. Potentials recorded from a central process of F3, third ganglion. Upper trace is intracellular record; lower trace is from ipsilateral ventral nerve cord, 2/3 connective. *A:* stimulation of the lateral giant in the 5/6 connective, at frequencies of 1, 10, and 100 Hz from left to right. Cord monitor records lateral giant discharge only; F3 axon spikes are absent. Each record shows several successive responses photographically superimposed. *B:* same as A, but with electrode withdrawn to just outside of F3. C_1, subthreshold, and C_2, suprathreshold antidromic stimulation of F3 in the ipsilateral third root of the third segment.

of identified neurons in invertebrate neuro-pil (28). The dorsal branches of fast flexor motoneurons were penetrated near their synapses with the lateral giant. The approximate location of the motoneuron processes is known from fluorescent dye injections and reconstructions of the motoneurons (12, 21). Single identified motoneurons were stimulated selectively by applying shocks to the appropriate branch of the third root of an abdominal ganglion (21a), and the focal potentials in the region surrounding motoneuron processes were used to direct the microelectrode to an identified motoneuron process.

Figure 3 shows the responses of a process of F3 to lateral giant stimulation. As stimulation progressed, the potential fractionated into all-or-none components. Since all of the potentials of Fig. 3 were unaccompanied by peripheral axon spikes, they are probably

branch spikes occurring in regions remote from the electrode site. Antidromic stimulation produced a full axon spike at the recording site (Fig. 3C), so the penetration was probably in the main axon, near the dendritic branches. The orthodromic potentials in Fig. 3A arise directly from the presynaptic giant neuron spike, whose field potential appears as a diphasic deflection inside the motoneuron (Fig. 3A), or just outside it (Fig. 3B). No synaptic delay is evident in the records.

Similar results were obtained from eight successful penetrations of different nongiant fast flexor motoneuron processes. Figure 4 presents the results of a penetration of F8. Orthodromic stimulation resulted in a full spike in the process penetrated, triggered by an underlying potential which began at the moment that the lateral giant spike passed the penetration site. The arrival instant of
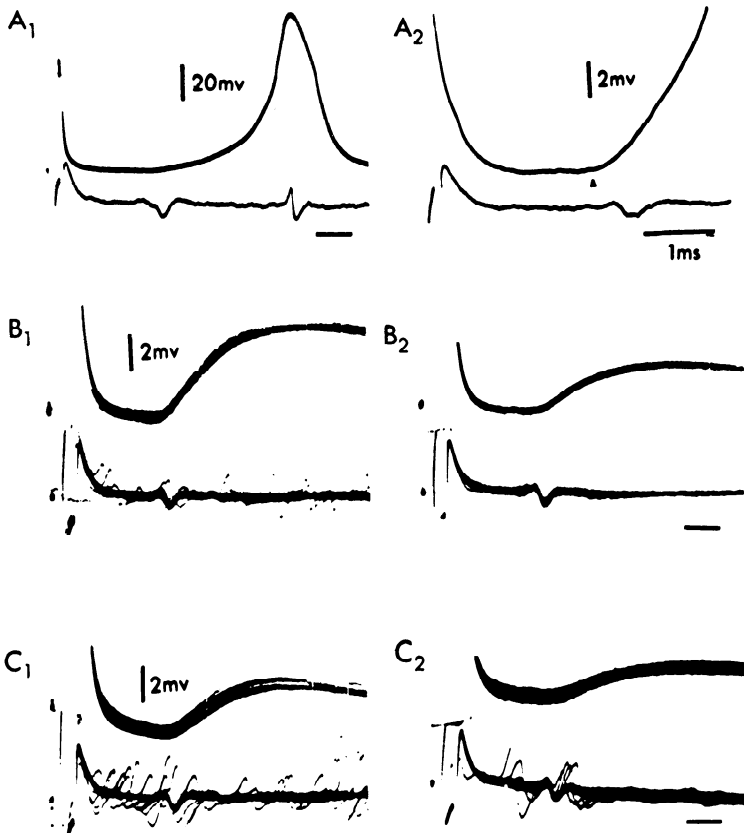
FIG. 4. Potentials recorded from a central process of F8, third ganglion. Electrodes and traces as in Fig. 3. A: lateral giant stimulation at 0.5 Hz. B: superimposed responses during the first (B_1) and fifth (B_2) second of orthodromic stimulation at 50 Hz. C: same as B, but the frequency is 100 Hz. Axon and dendrite spikes are blocked until only the EPSP remains.

the presynaptic impulse is indicated by a triangle in A_2; this time was calculated from the measured distances between the stimulating and cord-monitoring electrodes and the penetration site, as described earlier (28). Repeated stimulation at high frequency caused the axon spike to be blocked, and the underlying branch spike fell successively by discrete decrements until only a very small potential remained. This potential followed high-frequency orthodromic stimulation at constant amplitude for several minutes, and showed negligible synaptic delay; it therefore is interpreted as an electrically induced EPSP from the lateral giant to F8. The several all-or-none components intermediate between the EPSP and the axon spike are apparently branch spikes arising in the dendrites of the motoneuron and propagating variable distances down the dendritic tree toward the main axon. Note that the branch spikes and EPSP recorded from central processes (Figs. 3 and 4) are of briefer duration than those recorded from the soma (Figs. 1 and 2). In general, branch spikes recorded centrally (Figs. $3A$, $4B$) are larger than those recorded from the soma (Fig. $2A_2$).

Changing the level of polarization in the motoneuron process by 20 mv had no demonstrable effect on the size of the EPSP. This result does not eliminate the possibility of a component of chemical excitation of the motoneurons, however, because the electrode was some distance from the synapses on the distal dendrites. It is therefore unlikely that polarization of the motoneuron process would have any effect on chemical EPSPs, even if present.

The two lateral giant neurons are electrically coupled in each segment and normally fire together, and almost synchronously (24). Thus, if fast flexor motoneurons are driven electrically by the lateral giant fibers, then one might expect to observe synaptic potentials from both lateral giants in those motoneurons which are excited by each member of the pair, including F3 (12, 22, 22a). This complication was avoided in the experiments of Figs. 3 and 4, in which the lateral giant synchrony had been eliminated by prolonged repetitive stimulation of one giant, which is known to fatigue the cross connections between the lateral giant fibers (7, 24). In most experiments, however, both lateral giants fired nearly synchronously when either was stimulated, and the resultant EPSP was generated in part by activity in each giant. In Fig. 5B, for example, repetitive (50 Hz) orthodromic stimulation led to soma potentials in F3 that sometimes included a dendrite spike (large soma potential). When the dendrite spike failed to occur, an EPSP from the two giants remains in the left and center records. After prolonged stimulation of the ipsilateral giant fiber, the contralateral giant failed to respond. At the same time, the EPSP in F3 was reduced in all-or-none fashion (Fig. 5B, right), due to the loss of input from the contralateral giant fiber.

Similar results were obtained in all experiments in which the lateral giant synchrony could be overcome by fatigue.

The best criterion for establishing the electrical nature of a junction is to place microelectrodes on both sides of the junction for passing current and recording potentials, in order to measure the coupling resistance and properties of the synapse. This procedure has yielded convincing results in the case of the lateral giant electrical excitation of the motor giant neuron (7). This junction occurs in the nerve cord, where the motor axon crosses the giant axon near the third root. The synapses recorded in this paper are between the lateral giant axon and small motoneuron processes in neuropil (21), and simultaneous penetration of pre- and postsynaptic elements would be technically extremely difficult.

A test for unrectified coupling was performed by placing a recording microelectrode in the lateral giant axon where it contacts the fast flexor motoneuron processes. These motoneurons were then stimulated antidromically in the third root. Only a small diphasic focal potential could be seen in the giant axon; it grew from 0.1 to 0.5 mv as additional motoneurons were recruited antidromically by increasing the stimulus intensity. No sign of a monophasic positive backward coupling potential was observed. Several possible explanations of this result are available. One might suppose that the junction is rectifying, like that between the giant fiber and the motor giant (7). However, Bennett (1) has shown that just such an asymmetry between forward and backward coupling is expected whenever the presynaptic element is much larger in size (i.e., has a smaller input impedance) than the postsynaptic element, even if the coupling resistance does not rectify. The
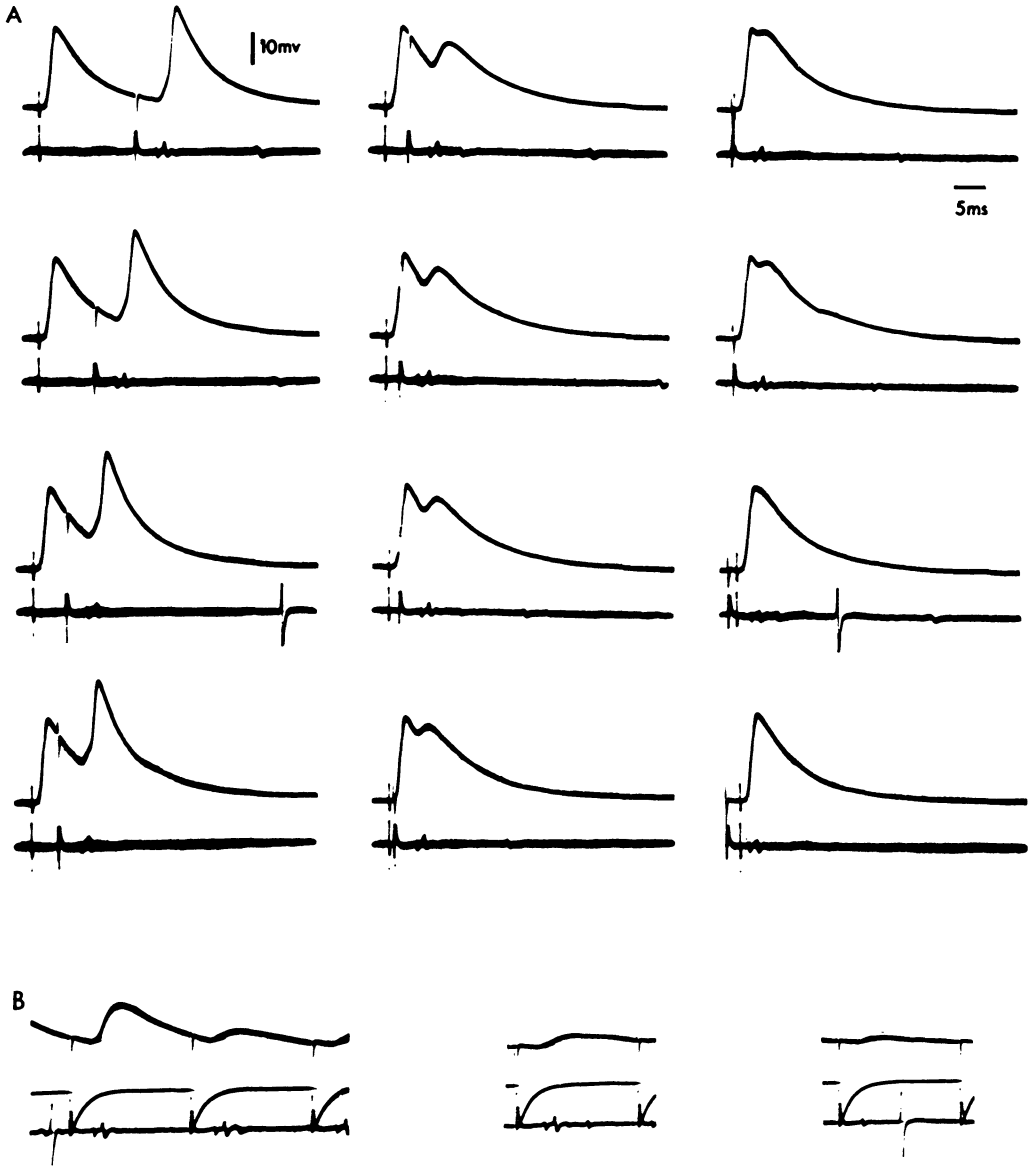
FIG. 5. *A:* interaction between antidromic and orthodromic soma potentials in F3, third ganglion. Upper trace is from the motoneuron soma; lower trace records from the ipsilateral nerve cord, 2/3 connective. Third root (antidromic) responses are associated with the small stimulus artifact; orthodromic responses were elicited by ipsilateral lateral giant stimulation in the 5/6 connective. The two nerve cord spikes following orthodromic stimulation represent activity in the two giant fibers. The stimulation sequence was repeated at 0.5 Hz, and the orthodromic response includes an axon spike at separations of greater than 6 msec. *B:* stimulation of the lateral giant alone at 50 Hz causes the axon spike to fail leaving only a dendrite spike (large potential) or EPSP (small potential). On the right, the contralateral giant fiber no longer responds to the stimulation. The middle trace is from the ipsilateral third root; other traces as in *A.*

anatomical evidence indicates such a large size asymmetry for these junctions (21). Finally, it is possible that axon discharges do not actively propagate antidromically into the motoneuron dendrites, and thus would never reach the locus of the synapse. The next section provides evidence that this third explanation is the most likely.

Interactions between axon and dendrite spikes

The ability to block soma, axon, and dendrite spikes selectively suggests that these discharges occur in separate regions connected by regions or structures of low safety factor. More evidence for this interpretation is presented in Fig. 5A. In this experiment, test orthodromic stimuli to the lateral giant were preceded by conditioning antidromic stimuli to the third root, and the soma potentials from F3 were recorded. When the interval between the responses to antidromic and orthodromic stimulation was greater than 6 msec, the orthodromic response included a component identical to the antidromic soma potential, which must therefore represent an axon spike. At shorter intervals, the axon spike was blocked, presumably by refractoriness, and orthodromic stimulation produced a component 1 soma potential. Figure 5B shows that this soma potential could be blocked in all-or-none fashion by high-frequency (50 Hz) stimulation of the giant fiber, and therefore appears to be a dendrite spike.

As the interval between the antidromic axon spike and orthodromic dendrite spike is reduced, the size of the dendrite spike declines gradually, until it is totally occluded by the axon spike when the potentials occur simultaneously. Figure 6 shows this result. If the antidromic axon spike were to invade the dendrites, it would be expected to block the following orthodromic dendrite spikes by refractoriness, and at brief intervals by collision. In this case, the orthodromic soma potential should be reduced by large discrete steps as it follows the axon spike more closely. This is never observed. If, however, the axon spike is blocked at some region of low safety factor, it will in turn be prevented from blocking dendrite spikes. The two potentials would be expected to sum very nonlinearly, since the membrane potential between the regions carrying the two discharges cannot be driven above the peak depolarization for either discharge. If the soma is connected passively to this intermediate region, it too should be depolarized by little more than the peak of the spike which most closely approaches the junction of the soma process and the axon-dendrite
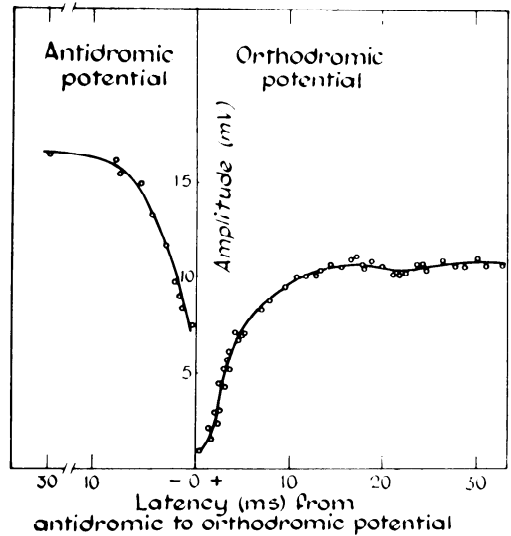
FIG. 6. Relation betcen amplitude of second potential and interval or latency between antidromic and orthodromic responses. Same experiment as Fig. 5. On the right, the orthodromic response follows the antidromic response, while on the left, the antidromic response is second.

process. These predictions are confirmed by the results shown in Fig. 6. The orthodromic dendrite spike thus adds only 1 mv to the antidromic axon spike when they are coincident.

In the previous experiment, the stimulation sequence was repeated once per 2 sec. Stimulating the lateral giant alone at 40 Hz caused the dendrite spike to fail about one time in three (see Fig. 5B). If an antidromic axon spike were blocked close to the dendrite instead of invading it actively, its electrotonic depolarization should leave the dendrite more excitable. As orthodromic stimuli follow an antidromic stimulus more closely, they should become increasingly likely to evoke dendrite spikes. This prediction is confirmed by the results shown in Fig. 7. The probability that an orthodromic soma potential includes a branch spike is plotted as a function of its separation from an antidromic axon spike. This result seems to confirm the conclusion that soma potentials intermediate between the axon spike and the EPSP are due to dendrite spikes.

Electrical model of motoneuron F3

In order to guess intelligently at the location of the processes carrying the axon and
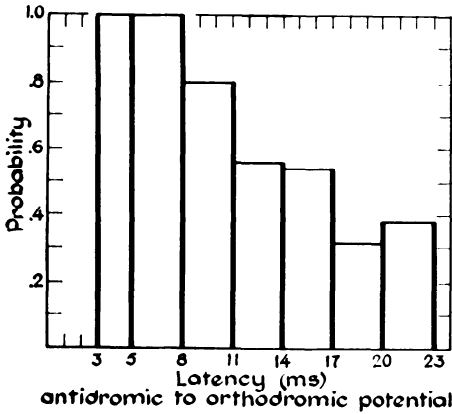
FIG. 7. Probability that the orthodromic potential includes a branch spike, as a function of the interval or latency by which it follows an antidromic response. Stimulation sequence repeated at 40 Hz.

dendrite spikes, and particularly their points of blockage, a physical model of motoneuron F3 was constructed using anatomical and electrophysiological data. A schematic drawing of the architecture of F3 is shown in Fig. 8A; the dimensions were obtained from a whole mount of a Procion yellow filling of neuron F3, and a reconstruction of its anatomy (21). Such a neuron may be abstractly represented as a branched

chain of compartments, where each compartment is equivalent to a small length of nerve process, or the soma (Fig. 8B). Since only the passive responses of the cell to spikes blocking at certain points will be considered, each compartment can be replaced by a resistor and capacitor in parallel, representing a segment of nerve membrane, and a series resistor between adjacent compartments, corresponding to the intracellular core resistances. The properties of such neural compartmental models have been explored extensively (19).

The procedure for choosing the values of the electrical components is as follows: An electrotonic length (Δz) is selected for each compartment:

$$\Delta z = \frac{\Delta l}{\lambda}$$

where λ is the space constant of the cylindrical process, and Δl is the length of each compartment. I used $\Delta z = 0.2$. Then the membrane resistor is

$$r = \frac{R_m}{\pi d \Delta l}$$

where d is the diameter of the process and R_m is the specific resistance of the nerve
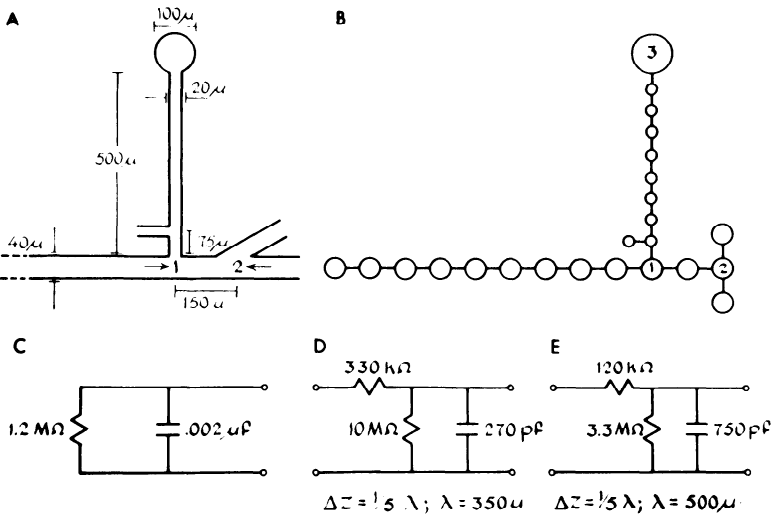
FIG. 8. Electrical model of fast flexor motoneuron F3. A: anatomy of the neuron. B: compartmental representation of neuron. C: soma compartment. D: soma process compartment. E: axon-dendrite compartment. 1: point where antidromic axon spike blocks. 2: point where orthodromic dendrite spike blocks. 3: point of recording soma potentials.

membrane of unit area. The membrane capacitor is

$$c_m = C_m \pi d \Delta l$$

where C_m is specific membrane capacitance per unit area. The axoplasm resistor is

$$r_i = \frac{4R_i \Delta l}{\pi d^2}$$

where R_i is the specific resistance of axoplasm or neural cytoplasm. The soma resistor and capacitor are $R_s = R_m/S$ and $C_s = C_m S$, where S is the surface area of the soma.

R_m may be calculated from the input resistance of the neuron measured from the soma, R_n, by the formula (see ref 17, equations 25, 26, 29, and 30):

$$R_m = \frac{\pi^2 d^3 R_n^2}{16 R_i} \left[1 + \sqrt{1 + \frac{16 R_i S}{\pi^2 d^3 R_n}} \right]^2$$

C_m may be derived from the measured time constant of the membrane, τ, by using $C_m = \tau/R_m$. No simple way exists for estimating R_i, and no report of axoplasmic resistivity in fresh water crustaceans could be found in the literature. Crayfish sarcoplasmic resistivity is reported to average between 125 and 203 ohms-cm (6, 8); I chose 164 ohms-cm for R_i in the above equations. Takeda and Kennedy (22) found R_n to be about 750 kilohms for nongiant fast flexor motoneuron somata, using one electrode for passing current and another for recording potentials. I obtained similar values for F3, using a bridge circuit. The time constant was reported (22) to be about 2.5 msec, and I also confirmed this value. The value was determined assuming an exponential response of the soma to a square-current step. Since the dendrites do not greatly dominate the input conductance at the soma ($\rho = 2$), this approximation does not introduce a serious error (18). Finally, space constants were calculated from the formula

$$\lambda = \sqrt{\frac{R_m d}{4 R_i}}$$

These measurements and equations were used to determine the values of the components of the model, shown in Fig. 8C, D, and E. This model assumes that the extra-

cellular resistivity is negligible. McAlister (15) has shown that this assumption has little effect on the internal potentials, compared to models in which a three-dimensional resistance network is used in each compartment to represent a volume conductor (see also ref 5).

Looking at the architecture of the neuron, and considering the results of the last section, it seems that the most likely points of low safety factor where spikes might block are the branch points indicated by the numerals 1 and 2 in Fig. 8A and B. At these points, a propagating action potential rapidly encounters a lower resistance due to the additional branch, and the increased load may lower the local circuit current in advance of the action potential below threshold (20). To test this hypothesis, intracellularly recorded action potentials from the F3 peripheral axon were imposed on the model at points 1 and 2, and the potentials at the soma recorded. The soma potentials predicted by the model to correspond to axon spikes and dendrite spikes are shown in Fig. 9. These potentials are remarkably
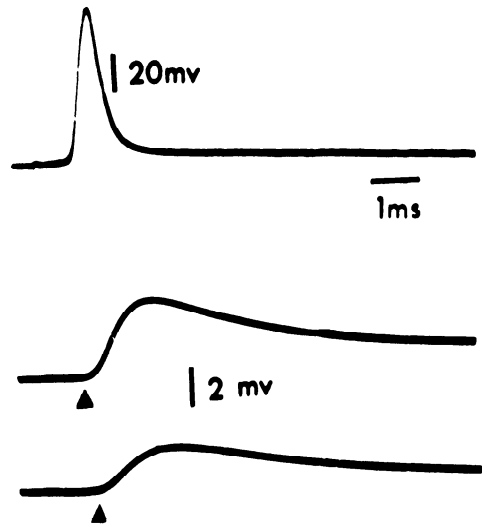
FIG. 9. Soma potentials predicted by the electrical model of Fig. 8. The model was driven by axon spikes recorded from F3, shown on the top trace. The middle trace shows the model soma potential in response to a spike imposed at the junction of the axon and the soma process (point 1 of Fig. 8). The last trace is the model soma potential caused by a spike imposed at the major dendrite branch point (point 2 of Fig. 8). Triangles mark the moment that the rising phase of the input spike begins.

TABLE 1. *Properties of predicted and observed soma potentials*

Properties	Dendrite Spikes		Axon Spikes	
	Predicted	Observed	Predicted	Observed
Apparent delay,* msec	0.25	0.2-0.4	0.18	0.1-0.2
Latency to peak,† msec	1.8	2-4	1.3	1.5-3
Half decay time,‡ msec	6.0	5-8	4.5	4-6
Amplitude at peak, mv	3.0	3-7	5.0	5-13

* Time between arrival of spike in presynaptic neuron and apparent foot of the potential at low amplifier gain. † Time from foot to peak of potential. ‡ Time from peak to half maximum of potential.

similar to the physiological soma potentials (cf. Figs. 1 and 2). Most noteworthy are the apparent delay of the foot of the potential, the broadened waveforms of the potentials, and the relative sizes and shapes of the axon and dendrite spikes seen from the soma. Table 1 compares the range of these properties of the F3 soma potentials recorded in 10 experiments to the predictions of the electrical model. Minor discrepancies between predicted and observed properties can easily be explained by the many assumptions involved in constructing the model (see DIS-CUSSION). It may be concluded that the physiological evidence for independent axon and dendrite spikes separated by regions of low safety factor corresponds to what is expected from the anatomical locations and dimensions of the axon, dendrites, soma process, and soma, and the branch points of the processes.

DISCUSSION

Lateral giant activation of motoneurons

The first finding is that fast flexor motoneurons of the crayfish abdomen are electrically excited by the lateral giant neurons. This conclusion is based on the high frequency stability and lack of synaptic delay of the EPSPs recorded in motoneuron central processes in response to giant fiber stimulation.

It is also possible that a component of chemical transmission is present between the lateral giant and the motoneurons, which might account for the sensitivity of these junctions to nicotine (26). One might expect such a component to appear as a delayed and slower depolarizing potential in motoneuron somata or processes, which declines gradually with rapidly repeated ac-

tivation, or as a potential whose amplitude is influenced by postsynaptic polarization. Such a component has never been seen but it would be difficult to observe from the usual distant site of electrode penetration, and would also be hard to discern because of the dendrite spikes intervening between the synapses and the electrode.

A further possible means of distinguishing electrical from chemical synapses is to observe the effect of high-Mg^{++} or low-Ca^{++} concentrations on the EPSP. At many neuromuscular junctions, and a few neuronal synapses, these ionic alterations depress chemical EPSPs by interfering with the presynaptic release of transmitter (see ref 28 for pertinent references). In several experiments, isosmotic solutions containing 11 times normal Mg^{++} (that is, 33 mM) and/or 15% normal Ca^{++} (2 mM) were used instead of normal Ringer. The responses in several fast flexor motoneuron somata to lateral giant stimulation were normal, which might be taken as evidence that these motoneurons are not chemically excited by the giant. This result, however, is unconvincing without a control experiment, demonstrating that these ionic treatments block known central chemical synapses in crayfish. Unfortunately, I have not been able to perform such a control successfully. For example, the lateral giant generates a large hyperpolarizing inhibitory postsynaptic potential (IPSP) in F10, the fast flexor peripheral inhibitor, which may be observed in the soma (21a). The long central delay and graded variable amplitude indicate that this polysynaptic IPSP is chemically mediated. Nevertheless, the IPSP was unaffected by soaking a desheathed abdominal nerve cord in high Mg^{++}-Ringer for 2 hr. Furthermore, the chemical synapses between tactile afferent and identified multisegmental tactile interneurons have been shown to be unaffected by solutions containing high Mg^{++} and low Ca^{++} (28). These negative results may be explained by supposing that there exists some impermeable diffusion barrier between

the ganglion surface and synapses located deep in dense neuropil. Finally, it has been shown that Ca++ deprivation can uncouple electrical junctions between neurons (16). It is clear that the procedure of bathing this preparation in solutions of altered ionic formulation reveals little about the nature of central synapses.

It is also not possible at present to use pharmacological blocking agents to selectively block a possible component of chemical transmission onto the motoneurons, since no central excitatory transmitters have so far been identified in crustacea.

The crayfish giant-to-motoneuron electrical junctions may provide a clue to the often-asked question: why are giant fibers giant? (4, 10). Bennett (1) has pointed out that the most effective electrical transmission occurs from large presynaptic elements. The presynaptic process in these synapses is the axon of the giant fiber (10, 12), and it may be that making the giant fiber giant is a way of ensuring that a single "decision fiber" can effectively excite spikes in a large number of postsynaptic motoneurons. The electrical mode of transmission seems to be used here, as elsewhere, to ensure synchrony in the firing of the motoneurons.

Dendrite spikes in motoneurons

The potentials in motoneuron somata which were subthreshold for generating axon spikes were first designated branch spikes by Takeda and Kennedy (22), because of their discrete amplitudes and susceptibility to blockage by hyperpolarization. The present results strengthen this hypothesis by showing that they are independent of axon spikes, and that their probability of occurrence is enhanced by preceding antidromic axon spikes, which never block dendrite spikes. The use of an electrical model to generate soma potentials similar to axon or branch spikes, depending on where the spike is thought to fail, provides additional evidence that these components of the soma potential are due to impulse blockade at points of low safety factor imposed by branching of motoneuron processes. The model correctly predicts most aspects of the physiological soma potentials.

Two properties of the predicted potentials differ significantly from the average experimental observations: the model potentials were too small and their rise times too short. There are several possible reasons for these slight discrepancies. For example, the measured input resistance of the motoneuron is probably below its real value due to the damage incurred by penetrating the soma with two electrodes. Furthermore, the value of axoplasm resistivity is chosen by analogy with reported values for sarcoplasm resistivity, which vary widely according to the source and between individuals. Thus it is probable that the electrotonic length of the soma process was overestimated in the model. In addition, the diameter of the soma may have been overestimated from dye-injected cells, because of histological swelling and a halo effect encountered in fluorescence microscopy. Thus the soma resistance was probably underestimated in the model. These sources of error act to reduce the magnitude of soma potentials generated by the model. In addition, the use of peripherally recorded axon spikes to generate model potentials tacitly assumes that the waveforms of dendrite and axon spikes are similar. Given the structural and dimensional similarities of the axon and proximal dendrites, this assumption seems reasonable, but is as yet unverified. A somewhat slower spike in the central processes would explain why the observed rise times were slower than the model predicted. A more serious error arises from the fact that a part of the rise of the soma potential is generated by axon or dendrite spikes before they have reached the point of block. This contribution of the propagating impulses to the soma potentials is ignored by the present simplified model.

The function of dendrite spikes is presumably to amplify the electrically induced EPSPs generated in distal dendrites so as to produce enough current to drive the main axon to threshold. At frequencies below 1 Hz, the dendrite spike usually leads to an axon spike. In some motoneurons, this process does not always occur, and only a small fraction of lateral giant discharges elicit postsynaptic axon spikes, even at low frequencies. For this reason, the electrical mode of transmission with branch spike amplification displays a variability usually associated with chemically mediated synaptic transmission. Thus, most lateral giant-evoked tail flips involve axon spikes in only a few of the fast flexor motoneurons excited subliminally by the giant (21a). This uncertainty of response of some of the motoneurons does not contribute visibly to the appearance of a critically viewed lateral

giant-evoked tail flip, however (14); these tail flips still look like all-or-none actions.

Fast flexor motoneurons are certainly not the only cells that generate dendrite spikes as part of a normal mode of orthodromic activation. Dendrite spikes have been recorded in a variety of neurons in the vertebrate brain, including cells in hippocampus, motor cortex, cerebellum, thalamus, and red nucleus (ref 9, p. 220), as well as in crayfish interneurons (11, 23).

SUMMARY

The modes of activation of the fast flexor motoneurons by the lateral giant were studied. Intracellular recordings from neuropil processes of identified motoneurons reveal an electrical component of excitation from the lateral giant. The electrical EPSP is normally amplified by a dendrite spike, which is necessary for the excitation of an axon spike in the motoneuron.

Conditioning antidromic axon spikes do not block dendrite spikes elicited orthodromically, either by collision or refractoriness; rather, they increase the probability that an orthodromic stimulus will evoke a dendrite spike. It is concluded that the axon spike invades the dendrite only passively.

The blocking of the antidromic axon spike and the orthodromic dendrite spike apparently occur at points of low safety factor in the motoneuron. An electrical model was built, representing the structure of a fast flexor motoneuron, employing morphological data obtained by dye injection. It predicted the form of motoneuron soma potentials due to axon and dendrite spikes which blocked at the major branch points of the neuron's processes.

REFERENCES

1. BENNETT, M. V. L. Physiology of electrotonic junctions. *Ann. N.Y. Acad. Sci.* 137: 509–539, 1966.
2. BENNETT, M. V. L. Similarities between chemically and electrically mediated transmission. In: *Physiological and Biochemical Aspects of Nervous Integration*, edited by F. D. Carlson. Englewood Cliffs, N.J.: Prentice-Hall, 1968, p. 73–128.
3. BRUNER, J. AND KENNEDY, D. Habituation: occurrence at a neuromuscular junction. *Science* 169: 92–94, 1970.
4. BULLOCK, T. H. AND HORRIDGE, G. A. *Structure and Function in the Nervous System of Invertebrates*. San Francisco: Freeman, 1965.
5. CLARK, J. AND PLONSEY, R. A mathematical evaluation of the core conductor model. *Biophys. J.* 6: 95–112, 1966.
6. FATT, P. AND GINSBORG, B. L. The ionic requirements for the production of action potentials in crustacean muscle fibres. *J. Physiol., London* 142: 516–543, 1958.
7. FURSHPAN, E. J. AND POTTER, D. D. Transmission at the giant motor synapse of the crayfish. *J. Physiol., London* 145: 289–325, 1959.
8. HENČEK, M. AND ZACHAR, J. The electrical constants of single muscle fibres of the crayfish

(Astacus fluviatilis). *Physiol. Bohemoslov.* 14: 297–311, 1965.
9. HUBBARD, J. I., LLINAS, R., AND QUASTEL, D. M. J. *Electrophysiological Analysis of Synaptic Transmission*. Baltimore: Williams & Wilkins, 1969.
10. KENNEDY, D. The comparative physiology of invertebrate central neurons. In: *Advances in Comparative Physiology and Biochemistry*, edited by O. Lowenstein. New York: Academic, 1966, vol. 2, p. 117–184.
11. KENNEDY, D. AND MELLON, DeF., JR. Synaptic activation and receptive fields in crayfish interneurons. *Comp. Biochem. Physiol.* 13: 275–300, 1964.
12. KENNEDY, D., SELVERSTON, A. I., AND REMLER, M. P. Analysis of restricted neural networks. *Science* 164: 1488–1496, 1969.
13. KENNEDY, D. AND TAKEDA, K. Reflex control of abdominal flexor muscles in the crayfish. I. The twitch system. *J. Exptl. Biol.* 43: 211–227, 1965.
14. LARIMER, J., EGGLESTON, A., MASUKAWA, L., AND KENNEDY, D. The different connections and motor outputs of lateral and medial giant fibres in the crayfish. *J. Exptl. Biol.* 54: 391–402, 1971.
15. MCALISTER, A. J. Analog study of a simple neuron in a volume conductor. *Naval Med.*

Research Inst. Research Rept. NM 01 05 00.01.01, 1958.

16. PENN, R. D. AND LOEWENSTEIN, W. R. Uncoupling of a nerve cell membrane junction by calcium-ion removal. *Science* 151: 88–89, 1956.

17. RALL, W. Branching dendritic trees and motoneuron membrane resistivity. *Exptl. Neurol.* 1: 491–527, 1959.

18. RALL, W. Membrane potential transients and membrane time constant of motoneurons. *Exptl. Neurol.* 2: 503–532, 1960.

19. RALL, W. Theoretical significance of dendritic trees for neuronal input-output relations. In: *Neural Theory and Modeling*, edited by R. F. Reiss. Stanford: Stanford Univ. Press, 1964, p. 73–97.

20. RUSHTON, W. A. H. Initiation of the propagated disturbance. *Proc. Roy. Soc. London, Ser. B* 124: 210–243, 1937.

21. SELVERSTON, A. I. AND KENNEDY, D. Structure and function of identified nerve cells in the crayfish. *Endeavour* 28: 107–113, 1969.

21a SELVERSTON, A. I. AND REMLER, M. P. Neural geometry and activation of crayfish fast flexor motoneurons. *J. Neurophysiol.* In press.

22. TAKEDA, K. AND KENNEDY, D. Soma potentials and modes of activation of crayfish motoneu-

rons. *J. Cellular Comp. Physiol.* 64: 165–182, 1964.

23. TAKEDA, K. AND KENNEDY, D. The mechanism of discharge pattern formation in crayfish interneurons. *J. Gen. Physiol.* 48: 435–453, 1965.

24. WATANABE, A. AND GRUNDFEST, H. Impulse propagation at the septal and commisural junctions of crayfish lateral giant axons. *J. Gen. Physiol.* 45: 267–308, 1961.

25. WIERSMA, C. A. G. Giant nerve fiber systems of crayfish. A contribution to comparative physiology of synapse. *J. Neurophysiol.* 10: 23–38, 1947.

26. WIERSMA, C. A. G. AND SCHALLEK, W. Influence of drugs on response of a crustacean synapse to pre-ganglionic stimulation. *J. Neurophysiol.* 11: 491–496, 1948.

27. WINE, J. J. AND KRASNE, F. B. The organization of escape behavior in the crayfish. *J. Exptl. Biol.* 56: 1–18, 1972.

28. ZUCKER, R. S. Crayfish escape behavior and central synapses. I. Neural circuit exciting lateral giant fiber. *J. Neurophysiol.* 35: 599–620, 1972.

29. ZUCKER, R. S. Crayfish escape behavior and central synapses. II. Physiological mechanisms underlying behavioral habituation. *J. Neurophysiol.* 35: 621–637, 1972.